

FLUKA ENERGY DEPOSITION STUDIES FOR THE HL-LHC*

L. S. Esposito[†], F. Cerutti, E. Todesco, CERN, Geneva, Switzerland

Abstract

The LHC upgrade, planned in about ten years from now, is envisaged to accumulate up to 3000 fb^{-1} integrated luminosity by running at a peak luminosity of $5 \times 10^{34} \text{ cm}^{-2} \text{ s}^{-1}$ [1]. In order to reach such an ambitious goal, the high luminosity insertions need a major redesign implying a 150 mm aperture low-beta Inner Triplet (IT), a superconducting D1 and new quadrupoles in the Matching Section. Energy deposition studies show that degradation of the coil insulator represents the most challenging issue from the radiation impact point of view. We propose a suitable shielding consisting of a beam screen with several mm tungsten absorbers at mid-planes to guarantee not to exceed a few ten MGy. This will also allow a good margin with respect to the risk of radiation induced quenches.

INTRODUCTION

The Large Hadron Collider (LHC) was operated at 4 TeV per beam and 70% of nominal luminosity in 2012. After the consolidation of the accelerator, it will provide 300 fb^{-1} integrated luminosity at $\sqrt{s} = 13 \div 14 \text{ TeV}$ within 2021. Subsequently, CERN is planning to make a high luminosity upgrade (HL-LHC) to get 3000 fb^{-1} in 10 years [1].

One essential objective of the upgrade is to reduce β^* by means of stronger and larger low- β triplet quadrupoles in the high luminosity Insertion Regions (IRs). The envisaged solution [2] relies on the new Nb₃Sn technology, which allows a more compact layout and $\sim 30\%$ higher performance with respect to Nb-Ti coils, and on a 150 mm aperture, doubling the present one of 70 mm. In addition, a super-conducting D1 separation dipole will replace the normal conducting version, and new quadrupoles in the Matching Section are foreseen, still based on Nb-Ti technology, but with larger aperture.

From the radiation damage point of view, these magnets should cope with an exceptional high luminosity. Therefore, they need to be designed to operate at $\mathcal{L} = 5 \times 10^{34} \text{ cm}^{-2} \text{ s}^{-1}$ (corresponding to 5 times nominal LHC peak luminosity), with a safe margin from their quench limit and have to resist to long term damage. Assumed quench limits [3, 4] are 12 (4) mW/cm³ for Nb₃Sn (Nb-Ti) coils, including a safety factor of 3. For radiation damage, a tentative dose limit is set to 30 MGy, mainly because of the degradation of the epoxy resin used to impregnate Nb₃Sn coils [5]. Another constraint is given by the total heat power to be evacuated from the ensemble of the IT, Corrector Package (CP) and D1 magnets by the cryogenic equipment. Recent work sets a design limit to 710 W [6].

* Research supported by the High Luminosity LHC project.

[†] Luigi.Salvatore.Esposito@cern.ch

The goal of this study is to evaluate power and dose on the coils of the magnets in the high luminosity IRs up to D1, and to propose a solution for an adequate protection.

BEAM LINE MODEL

The HL-LHC beam line has been modelled in FLUKA [7, 8]. The machine model can be built automatically from LHC optics files once the description of the geometry, materials and magnetic field is available for each component [9]. Round beam optics configurations have been used with $\beta^* = 15 \text{ cm}$ and $295 \mu\text{rad}$ half-crossing angle in the case of vertical (and horizontal) crossing plane [10]. All main elements from IP up to D1 have been modelled:

- a 1.8 m long TAS (Target Absorber of Secondaries) with 60 mm aperture;
- six IT quadrupoles with 150 mm coil aperture arranged in two pairs (Q1 and Q3) with 4.0 m long twin magnets, and a pair of 6.8 m long magnets (Q2A and Q2B);
- three 150 mm aperture orbit correctors, MCBX, with nested Nb-Ti coils to provide both a vertical and horizontal kick: two 1.2 m long magnets placed before Q2A and after Q2B, respectively, and a 2.2 m one located in the CP;
- nine 150 mm aperture super-ferric magnets [11] (a skew quadrupole and eight high order multiples, from sextupole to dodecapole, normal and skew) hosted in the CP downstream Q3;
- one 6.36 m long dipole with 160 mm aperture Nb-Ti coil.

The beam line aperture is shown in Fig. 1. The optics configuration of the IT quadrupoles Q1-Q2A-Q2B-Q3 is DFFD¹ in the vertical plane for the outgoing beam.

To protect IR elements from collision debris particles, we consider an octagonal beam screen with 6 mm tungsten absorbers on the mid-planes along the IT, the CP and the D1, except in Q1 where the assumed thickness is 16 mm, taking advantage of less tight optics constraints on the aperture. Figure 2 shows the two beam screen versions, where the absorbers attached outside are not in thermal contact with the cold mass. From the point of view of energy deposition, the beam screen function is two-fold: 1) it reduces the peak energy deposition in the coils; and 2) it removes a sizeable part of the heat load from the 1.9 K cooling system. Present HL-LHC layout foresees six cryostats to host all aforementioned magnets: four cryostats for IT magnets (Q1, Q2A, Q2B and Q3), one for the CP and the last one

¹F stands for focusing, D for defocusing.

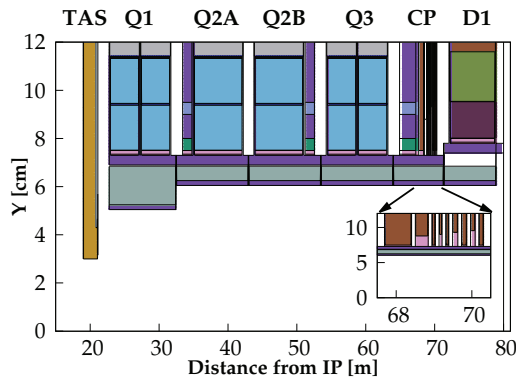


Figure 1: HL-LHC beam line aperture from TAS to D1. The inset shows a magnification over the position of the super-ferric magnets hosted in the CP cryostat.

for the D1. Over the interconnects, the distance between the magnets is $1.5 \div 1.7$ m. This represents a vulnerable point in the shielding, since an interruption of the beam screen is necessary therein. As a first tentative baseline, we assume 100 mm interruption of the beam screen in the middle of the interconnects.

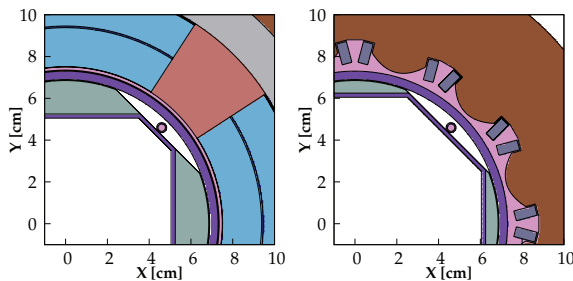


Figure 2: Magnet cross sections showing the beam screen with 16 mm tungsten absorbers in the Q1 (left) and with 6 mm absorbers in the normal dodecapole (right). 0.5 mm clearance is considered between the absorbers and the beam screen.

Collision debris particles coming from inelastic and diffractive interactions at the IP have been simulated using the FLUKA built-in interface to DPMJET III [12]. Beam divergence ($\sigma_{\theta_{x,y}} \approx 47 \mu\text{rad}$) and longitudinal vertex position distributions ($\sigma_z = 7.5$ cm) have been implemented. For the final normalisation, we assumed 85 mb proton-proton cross-section [13].

DOSE AND POWER ESTIMATES

The energy deposition density in the coils is scored using a 3D cylindrical mesh with about 10 cm longitudinal bins, 2-degree azimuthal bins. Steady-state heat loads are estimated by the peak power density ϵ_{max} averaged over the radial dimension of the inner coil layer (17, 16 and 10 mm for IT quadrupoles, D1 and orbit correctors, respectively, and ranging between 6 mm to 22 mm in the super-ferric correctors) to assess the risk of quench. Radiation dam-

age is determined by the peak dose D_{max} on a finer radial binning (3 mm), since relevant material degradation can be more localised, with heat diffusion playing no role in this respect.

Figure 3 shows the obtained ϵ_{max} and D_{max} longitudinal profiles. The patterns are dominated by the peak located at the end of Q1/beginning of Q2A and by the rise starting in the middle of Q2A, driven by the strong IT field. For super-ferric magnets in the CP, the peak power barely reaches 1 mW/cm^3 , and peak dose is lower than in the upstream orbit corrector hosted in the same cryostat. A comparison with the horizontal case is shown in Fig 4. For a DFFD configuration of the IT in the vertical plane, debris particle capture is more efficient if crossing is vertical, since particles leaving IP fly preferentially on this plane toward IR elements. Low momentum particles, already scattered on the vertical plane, are immediately caught by Q1 (defocusing). It turns out that D_{max} is the most crucial parameter for magnet design, since power deposition is well below the expected quench limit (by almost one order of magnitude in the Nb_3Sn case). Total heat loads deposited on the magnet cold masses and on the beam screen are reported in Table 1. It is worth to mention that one half of the heat load is removed by the beam screen. In case of horizontal crossing, integral values are about 10% lower. The margin in D1 might allow to consider a smaller aperture (150 mm, as per Inner Triplet magnets).

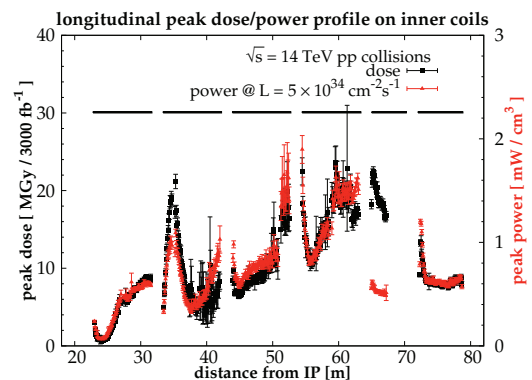


Figure 3: Longitudinal profile of D_{max} (boxes) and ϵ_{max} (triangles) along the IT quadrupoles, the CP and the D1 in the case of vertical crossing. Horizontal lines indicate the total magnetic lengths of the elements inside the same cryostats.

ROLE OF THE SHIELDING THICKNESS AND INTERCONNECT GAP

The thickness of the tungsten absorbers plays a crucial role in the magnet shielding, as it is shown in Fig. 5 where the baseline configuration is compared to the case with 8 mm absorbers in Q1B. The peak dose increases by about a factor of 3 in the concerned magnet, and the shadow effect on downstream element is reduced.

An increase of the beam screen gap length (from 10 to

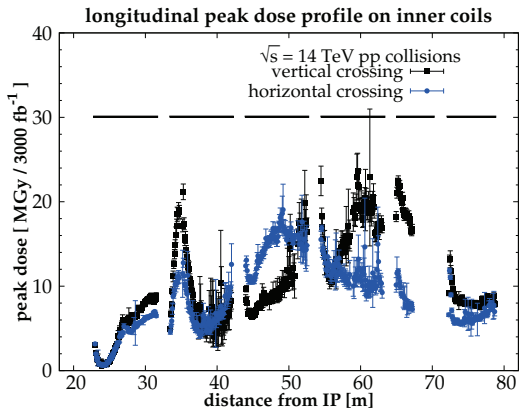


Figure 4: Longitudinal profile of D_{max} : vertical (boxes, as per Fig. 3) and horizontal (circles) crossing.

Table 1: Total head load aggregated by elements in the same cryostat for the vertical crossing. First column corresponds to total power on the magnet cold mass, second column is the budget removed by the beam screen.

	Magnet cold mass Power [W]	Beam screen Power [W]
Q1A+Q1B	100	175
Q2A+orbit corr.	95	60
Q2B+orbit corr.	115	80
Q3A+Q3B	140	80
CP	55	55
D1	90	60
Total	595	510

50 cm) has also an appreciable effect on the downstream element, which can be as high as a factor of 2. However, for the case shown in Fig. 5, the increase is mitigated by the shadow of the thicker beam screen in Q1B.

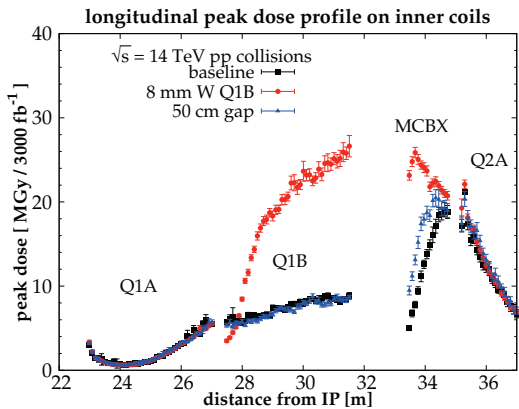


Figure 5: D_{max} longitudinal profile from Q1A up to Q2A: baseline scenario (boxes, as per Fig. 3) is compared to the cases with 8 mm tungsten absorbers in Q1B (circles), and with 50 cm beam screen gap in the interconnect (triangles).

CONCLUSIONS

In this study we considered a shielding option of the IR magnets that guarantees present HL-LHC goals (3000 fb^{-1} with a peak luminosity of $5 \times 10^{34} \text{ cm}^{-2}$). A beam screen with 6 mm tungsten absorbers at mid-planes along the Inner Triplet magnets (except in Q1, where we assumed 16 mm) up to D1, fulfils energy deposition requirements, especially in terms of long term radiation damage. Special attention should be devoted to the design of the interconnects.

ACKNOWLEDGMENTS

We would like to thank R. De Maria, S. Fartoukh for valuable discussions on beam optics, and P. Ferracin, T. Nakamoto, F. Toral and Q. Xu for essential inputs on magnet models.

REFERENCES

- [1] O. Brüning, L. Rossi, “High Luminosity Large Hadron Collider: A description for the European Strategy Preparatory Group,” CERN ATS 2012-236.
- [2] E. Todesco et al., “Design Studies for the Low-beta Quadrupoles for the LHC Luminosity Upgrade,” CERN-ATS-2013-018.
- [3] N. V. Mokhov et al., “Protecting LHC IP1/IP5 Components Against Radiation Resulting from Colliding Beam Interactions,” CERN-LHC-Project-Report-633.
- [4] N. V. Mokhov, I. L. Rakhno, “Mitigating radiation loads in Nb₃Sn quadrupoles for the CERN Large Hadron Collider upgrades,” Phys. Rev. STAB 9 (2006) 101001.
- [5] Composite Technology Development, Inc., Data-sheets.
- [6] J. M. Poncet et al., “Cooling options for the LHC high luminosity upgrade final focusing magnets,” to be published in Proc. CEC-ICMC, Anchorage, Alaska, 2013.
- [7] G. Battistoni et al., “The FLUKA code: Description and benchmarking,” AIP Conf. Proc. **896** (2007) 31. A. Ferrari et al., “FLUKA: A multi-particle transport code (Program version 2005),” CERN-2005-010.
- [8] V. Vlachoudis, “FLAIR: A Powerful But User Friendly Graphical Interface For FLUKA,” Proc. Int. Conf. on Mathematics, Computational Methods & Reactor Physics, Saratoga Springs, New York, 2009.
- [9] A. Mereghetti et al., “The FLUKA LineBuilder and Element DataBase: Tools for Building Complex Models of Accelerator Beam Lines”, IPAC2012, New Orleans, May 2012, WEPPD071, p. 2687 (2012).
- [10] R. De Maria et al., “HLLHCv1.0: HL-LHC Layout and Optics Models for 150 mm Nb₃Sn Triplets and Local Crab-cavities,” TUPFI014, these proceedings.
- [11] F. Toral et al., “Development of Radiation Resistant Superconducting Corrector Magnets for LHC Upgrade,” Applied Superconductivity, IEEE Transactions on, vol. **23**, 2013.
- [12] S. Roesler et al., “The Monte Carlo event generator DPMJET-III,” hep-ph/0012252.
- [13] J. Beringer et al., “Review of Particle Physics”, Phys. Rev. D **86**, 010001 (2012).